

# Dependence of the critical current of $\text{YBa}_2\text{Cu}_3\text{O}_{7-\delta}$ coated conductors on in-plane bending

D C van der Laan and J W Ekin

Department of Physics, University of Colorado, Boulder, CO 80309, USA  
and

National Institute of Standards and Technology, Boulder, CO 80305, USA

E-mail: [danko@boulder.nist.gov](mailto:danko@boulder.nist.gov)

Received 8 July 2008, in final form 6 August 2008

Published 3 September 2008

Online at [stacks.iop.org/SUST/21/115002](http://stacks.iop.org/SUST/21/115002)

## Abstract

A new method to measure the effect of in-plane bending on the critical current of  $\text{YBa}_2\text{Cu}_3\text{O}_{7-\delta}$  coated conductors is presented. Such a bending mode can be important in transmission cables, saddleback magnets, and double-pancake windings. A linear strain distribution over the width of the conductor develops in this bending mode, where one half of the conductor is under axial compressive strain and the other half is under axial tensile strain. A reversible reduction in critical current of up to 5% is measured in 4 mm wide conductors at a critical bending radius of 0.25–0.28 m. The critical current degrades irreversibly for bending radii less than this because the strain at the edge of the conductor that is under tension irreversibly damages the conductor. The results are described by use of a model that calculates the critical current as a function of in-plane bending radius by taking into account the strain gradient over the width of the sample and the measured dependence of the critical current on axial strain. A similar approach can be used to calculate the degradation of the critical current in other deformation modes, such as torsion, or other more complex geometries.

## 1. Introduction

Remarkable progress in the development of  $\text{YBa}_2\text{Cu}_3\text{O}_{7-\delta}$  (YBCO) coated conductors has been achieved in recent years, where very high critical current densities ( $J_c$ ) of 2.5–3.0 MA cm<sup>-2</sup> at 77 K have been reached in long conductor lengths [1]. The high degree of grain alignment that resulted in these high values of  $J_c$  has also resulted in a large improvement in the mechanical strength of coated conductors. The irreversible strain limit now exceeds 0.6% in axial tension [2]. With the improved mechanical strength and high degree of grain alignment, it has become apparent that it is not just the irreversible strain limit (the strain at which cracks develop that permanently interrupt current flow in the YBCO layer) that is important. Also, the reversible change in  $J_c$  as a function of axial strain has become an important design consideration for applications. Coated conductors may experience not only axial strain but also in-plane bending strain in applications such as transmission lines, saddleback magnets, and connections

between double-pancake windings. Although research has been performed on the effect of in-plane bending on other materials [3, 4], no data have been published regarding this effect in YBCO coated conductors.

The results of a new experiment are presented, where the change in critical current ( $I_c$ ) with in-plane bending is measured. A model that accurately calculates the effect of in-plane bending from uniaxial strain measurements is introduced. This model can be used as an engineering tool for the general design of applications under various deformation methods.

## 2. Experimental details

Different YBCO coated conductors that are produced by various methods were investigated. The first type consisted of ceramic buffer layers deposited on a 50  $\mu\text{m}$  thick Hastelloy C-276 substrate, where the YBCO layer is deposited on top of the buffer layers by metal-organic chemical-vapor deposition

**Table 1.** Conductor details.

Process	$J_c$ at 76 K (MA cm <sup>-2</sup> )	YBCO thickness ( $\mu\text{m}$ )	Added copper
MOCVD-1	MOCVD-IBAD 2.5	1.0	Plated
MOCVD-2	MOCVD-IBAD 2.7	1.5	Plated
MOCVD-3	MOCVD-IBAD 2.3	2.5	Plated
MOD-1	MOD-RABiTS 2.6	0.8	None
MOD-2	MOD-RABiTS 2.6	0.8	Laminated

(MOCVD) [5, 6]. Grain alignment is introduced into the MgO buffer layer by ion-beam-assisted-deposition (IBAD). Coated conductors of this type (MOCVD-IBAD) have a columnar YBCO grain structure. A silver cap layer 2 to 3  $\mu\text{m}$  thick is deposited on top of the YBCO layer for electrical and thermal stability. The coated conductors are then slit from a 12 mm wide tape to their final width of 4 mm. They are surrounded with 20  $\mu\text{m}$  of copper for electrical and thermal stability. The thickness of the YBCO layer varies between 1.0 and 2.5  $\mu\text{m}$ . Details of the conductor are listed in table 1.

The second type of coated conductor consisted of a YBCO layer 0.8  $\mu\text{m}$  thick deposited onto a grain-aligned substrate by metal-organic deposition (MOD) [7, 8]. This technique results in a laminar YBCO grain structure with meandering grain boundaries [9]. Grain alignment is introduced within a textured NiW substrate 75  $\mu\text{m}$  thick by use of the rolling-assisted biaxially textured-substrate (RABiTS) technique [10, 11]. These samples are designated MOD-RABiTS. The conductors were slit from a 4 cm wide tape to their final width of 4 mm. Several of the 4 mm wide MOD-RABiTS tapes were then also laminated with two copper strips 50  $\mu\text{m}$  thick by soldering the strips to the slit tape with 62 wt%Sn–36 wt%Pb–2 wt%Ag solder at over 179 °C. Sample details are listed in Table 1.

The dependence of the critical current on axial strain was measured at 76 K with a Cu–2 wt%Be beam in a four-point bending apparatus. Axial strain was applied to the sample, which was soldered onto the surface of the beam by use of In–3 wt%Ag solder with a melting temperature of 143 °C, as illustrated in figure 1 [2]. Axial tensile strain is applied to the sample when the beam is bent down, as shown in figure 1(a). When the beam is bent up, the sample is put under axial compressive strain, as shown in figure 1(b). The critical current was determined with an electric-field criterion of 1  $\mu\text{V cm}^{-1}$  and an uncertainty of about  $\pm 0.5\%$ . The axial strain in the 0.8–2.5  $\mu\text{m}$ -thick YBCO layer of the various samples was measured with a strain gage and was homogeneous over the thickness of the YBCO film to within 1 part in 1900–5900 (ratio defined by the thickness of the YBCO layer and the distance of the layer from the neutral axis of the beam). Current sharing with the CuBe bending beam was monitored with a second set of voltage tabs. The current through the beam was limited due to the resistive buffer layers that separate the YBCO layer from the metal substrate of the coated conductor. This shared current was significantly less than the uncertainty of the critical current.

The same bending beam and four-point bender were used to measure the effect of in-plane bending on the critical current, except that in this case the sample was soldered on the side

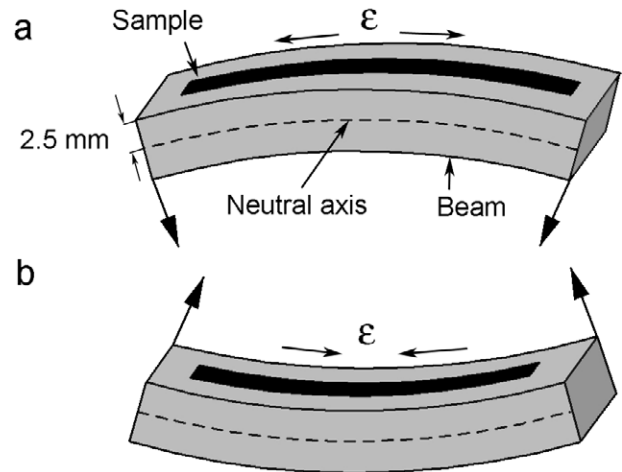


**Figure 1.** Illustration of the method for applying large axial strains to the superconducting sample, which is soldered on top of a Cu–2 wt%Be bending beam. Axial tension is applied by bending the beam in the direction shown in (a), whereas axial compression is applied by bending the beam in the opposite direction (b).

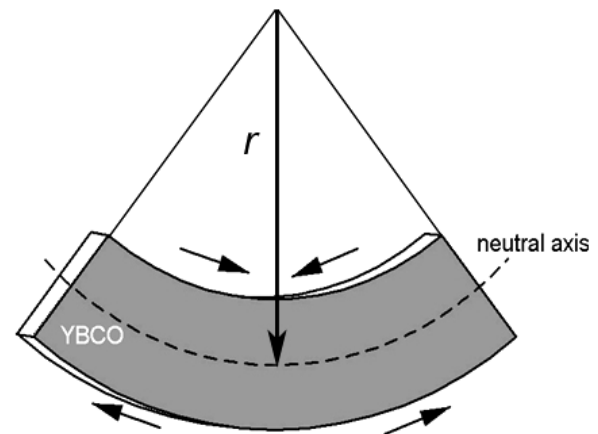


**Figure 2.** Illustration of a coated conductor under in-plane bending. The in-plane bending radius  $r$  is the radius of the neutral axis in the center of the sample. The arrows indicate which part of the sample is under axial tension and which is under axial compression.

of the beam, as shown in figure 2. The critical current was determined with the same electric-field criterion as a function of in-plane bending radius  $r$  (defined in figure 2). The bending radius was calculated from the strain that is measured on the top and bottom surfaces of the beam with strain gages. One half of the tape width is under axial tension, while the other half is under axial compression when the sample is bent in-plane, as illustrated in figure 2. The center of the sample where both regions of opposite strain meet is strain free. This region is designated the neutral axis of the sample.

### 3. Theory

The critical current density of YBCO coated conductors is highly dependent on axial strain. When uniform axial strain is applied to a coated conductor, the critical current density

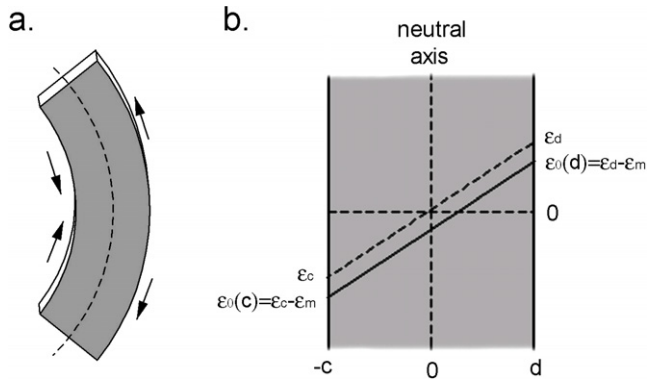


**Figure 3.** (a) A coated conductor that is bent in-plane. (b) The strain profile over the width of the conductor.

follows a power-law dependence on axial strain [2]. A non-constant spatial distribution in strain develops when a coated conductor is bent in-plane. The distribution in strain is a linear function of position over the width of the YBCO film and depends on the bending radius  $r$ . Figure 3(a) shows a coated conductor under in-plane bending, and the spatial distribution in strain over the width of the tape is shown in figure 3(b).

With the  $x$ -axis along the width of the conductor, the conductor edges are defined at  $-c$  and  $d$ , and the neutral axis where the applied strain is zero is located at  $x = 0$ . The values for  $c$  and  $d$  that define the width of the current path depend on how accurately the sample is soldered at the precise center of the bending beam, as well as how much damage from conductor slitting is present near the edges. These parameters are fitting parameters and are not determined experimentally. The slitting process may damage the YBCO near the edges, which will narrow the overall current path. In figure 3, the YBCO layer on the left side of the neutral axis is under compressive strain, while the part on the right of the neutral axis is under tension. The applied strain in the YBCO layer is a linear function of position (indicated by the dashed line), ranging from  $-\varepsilon_c(r)$  at the edge under compression to  $\varepsilon_d(r)$  at the edge under tension:

$$\varepsilon_c(r) = \frac{-c}{r} \quad (1a)$$

and

$$\varepsilon_d(r) = \frac{d}{r}. \quad (1b)$$

The strain that the YBCO layer experiences (the intrinsic strain  $\varepsilon_0$ ) is different from the applied strain, simply because the YBCO layer is placed under compressive strain when the sample and beam are cooled to low temperature. The extra compressive pre-strain  $\varepsilon_m$  is of the order of  $-0.1\%$ , as measured in the axial strain experiment. It shifts the intrinsic strain profile in the conductor to a slightly lower strain, as indicated by the solid line in figure 3(b).

The critical current of a coated conductor as a function of in-plane bending radius can now be calculated from the measured axial strain dependence by integrating the critical current density over the width of the sample, taking the linear

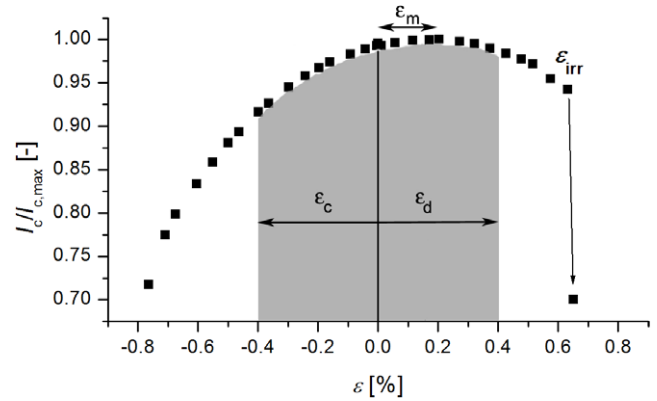


**Figure 4.** Critical current as a function of applied axial strain. The shaded area under the curve indicates the strain range that the 4 mm wide conductor experiences under in-plane bending at a bending radius of 0.5 m.

strain profile into account:

$$I_c(r) = \int_{-\varepsilon_c(r)}^{\varepsilon_d(r)} \frac{I_c(\varepsilon)}{\varepsilon_d(r) - \varepsilon_c(r)} d\varepsilon, \quad (2)$$

with

$$I_c(\varepsilon) = I_c(0) (1 - a|\varepsilon - \varepsilon_m|^{2.2}). \quad (3)$$

Equation (3) represents the measured dependence of  $I_c$  on applied axial strain  $\varepsilon$  in coated conductors (taken from [2]) where  $I_c(0)$ ,  $a$ , and  $\varepsilon_m$  are variables that depend on sample configuration and processing method. By taking independent values for the strain at both sample edges (by not setting  $\varepsilon_c$  and  $\varepsilon_d$  to be equal) this model is capable of predicting the critical current even if the neutral axis is not in the center of the sample, and when the extent of the slitting damage is not the same on each side.

The integral represented by equation (2) is basically the surface under the  $I_c$ - $\varepsilon$  curve (equation (3)) between the bending strain values at the edges  $-\varepsilon_c$  and  $\varepsilon_d$ , normalized to the absolute strain range that is present in the sample. This is illustrated by the shaded area in figure 4 shown under a typical axial  $I_c$ - $\varepsilon$  curve. The width of the shaded area grows when the in-plane bending radius becomes smaller, while the center of the shaded area remains at the neutral axis ( $\varepsilon = 0$ ) corresponding to the initial compressive pre-strain  $\varepsilon_m$ .

For instance, at a bending radius of 0.5 m for a 4 mm wide tape, the shaded area covers the strain range from  $-0.4\%$  at the edge under compression to  $0.4\%$  at the edge under tension.  $I_c$  is predicted to decrease irreversibly at a bending radius where the strain at the edge under tension exceeds the irreversible strain limit  $\varepsilon_{irr}$  ( $0.65\%$  as measured in pure axial strain tests, which corresponds to an in-plane bending radius of 0.31 m). A critical in-plane bending radius can thus be defined as the bending radius at which the strain at the edge under tension is equal to the irreversible strain limit:

$$r_{irr} = \frac{w}{2\varepsilon_{irr}}. \quad (4)$$

Here  $w$  is the width of the sample and  $\varepsilon_{irr}$  is the irreversible strain limit in axial tension.

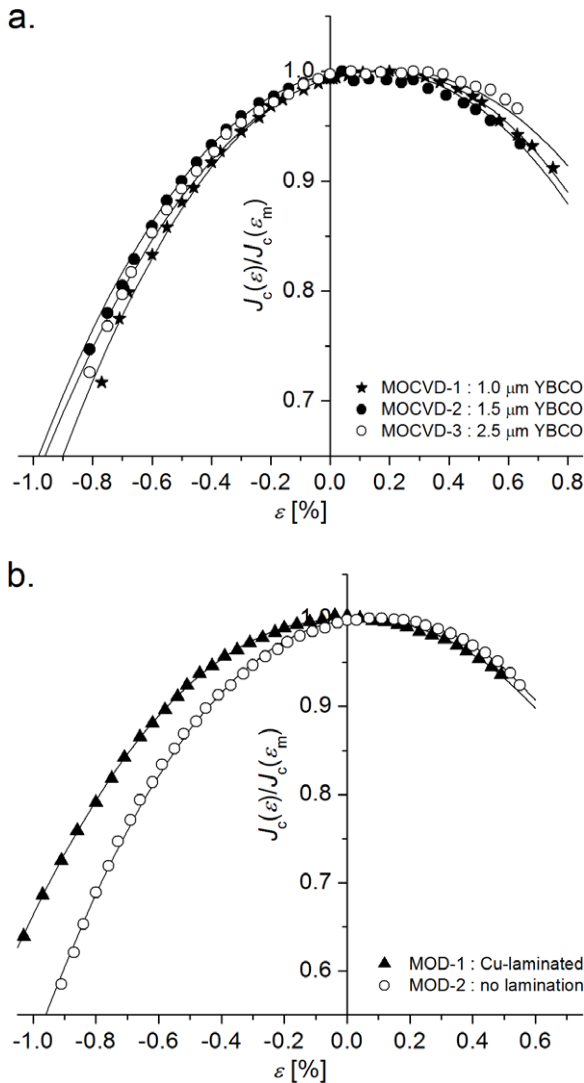


**Figure 5.** Normalized critical current density as a function of applied axial strain of (a) MOCVD-IBAD coated conductors with layer thickness of 1.0  $\mu\text{m}$  (MOCVD-1), 1.5  $\mu\text{m}$  (MOCVD-2) and 2.5  $\mu\text{m}$  (MOCVD-3) and (b) of MOD-RABiTS coated conductors with (MOD-2) and without copper laminates (MOD-1). The solid lines are a fit to the data according to equation (3).

#### 4. Results and discussion

Two samples from the same batch were measured for each type of YBCO coated conductor under investigation. The dependence of  $J_c$  on in-plane bending was measured for one sample, while the dependence of  $J_c$  on axial strain was measured for the other sample. The dependence of  $J_c$  on axial strain of three MOCVD-IBAD samples with different YBCO layer thicknesses (see table 1) is shown in figure 5(a). Here, the normalized critical current density is plotted as a function of applied strain. The critical current density is normalized to its maximum value, which occurs at an applied strain of  $\epsilon_m$ . The sample was first taken into compression, while  $J_c$  was measured for each strain step. At 0.8% compressive strain,  $J_c$  decreased reversibly by about 30%. After 0.8% compression was applied, the sample was taken into tension. The change in critical current density is reversible until the strain exceeds

**Table 2.** Parameter values for expressions (1) and (3).

	From axial strain measurements			Parameters for in-plane bending	
	$a$	$\epsilon_m$ (%)	$\epsilon_{irr}$ (%)	$c$ (mm)	$d$ (mm)
MOCVD-1	7000	0.14	0.75	2.1	1.6
MOCVD-2	6900	0.14	0.64	1.5	2.7
MOCVD-3	6500	0.15	0.63	1.4	2.4
MOD-1	8700	0.01	0.49	1.8	1.7
MOD-2	9900	0.05	0.55	1.3	1.9

the irreversible strain limit, which ranges from 0.6% to 0.8%. The data for irreversible reduction of  $J_c$  are not shown in the figure; only reversible data are shown. The dependence of  $J_c$  on applied strain is very similar, even for conductors with YBCO layers of different thicknesses. Also, the strain ( $\epsilon_m$ ) at which the peak in  $J_c$  occurs is comparable for various samples. The difference in thermal expansion coefficient between the YBCO layer, the metallic components of the sample, and the bending beam results in a pre-compression of the YBCO layer of about 0.2% ( $\epsilon_m$ ), when the sample and beam are cooled down from soldering temperature to 76 K. The solid lines in the figure were determined from equation (3) and fit the data well. The values of the parameters in expression (3) are listed in table 2.

The dependence of  $J_c$  on strain is also measured for two MOD-RABiTS coated conductors. The results for normalized  $J_c$  versus applied strain are shown in figure 5(b), together with a fit according to equation (3). The difference between the two samples is that sample MOD-2 is laminated with two copper strips. The difference in thermal expansion coefficient between the copper laminates and the YBCO layer causes the maximum in  $J_c$  to occur at a higher applied strain in sample MOD-2 compared to that of the non-laminated sample MOD-1.

The normalized critical current density of coated conductors MOCVD-1, MOCVD-2, and MOCVD-3 as a function of in-plane bending radius  $r$  is shown in figure 6(a).  $J_c$  is normalized to its value before the sample is bent in-plane. A very small (0.05%) reversible reduction in  $J_c$  is measured when the in-plane bending radius is reduced to below 1 m. The reversible reduction in  $J_c$  becomes larger when the bending radius approaches 0.5 m. The distribution in  $J_c$  at this bending radius is shown by the shaded area in figure 4. The critical current density at the edge under compression is reduced by almost 10%, while  $J_c$  at the edge under tension is reduced by less than 5%. When the in-plane bending radius is reduced further, the gray area in figure 4 grows in both directions, and a larger reversible reduction in  $J_c$  is measured. A reversible reduction in the overall  $J_c$  of 4–5% is measured at an in-plane bending radius of 0.25–0.28 m, depending on the sample. When the in-plane bending radius is reduced further, an irreversible change in  $J_c$  is measured, since the edge that is under tension is taken beyond the irreversible strain limit and the YBCO layer starts to crack. For clarity the data in figure 6 include only reversible data.

The dependence of  $J_c$  on in-plane bending for the two MOD-RABiTS coated conductors is shown in figure 6(b), which illustrates similar behavior to the MOCVD-IBAD samples. The solid lines in both figures are a fit to the data,

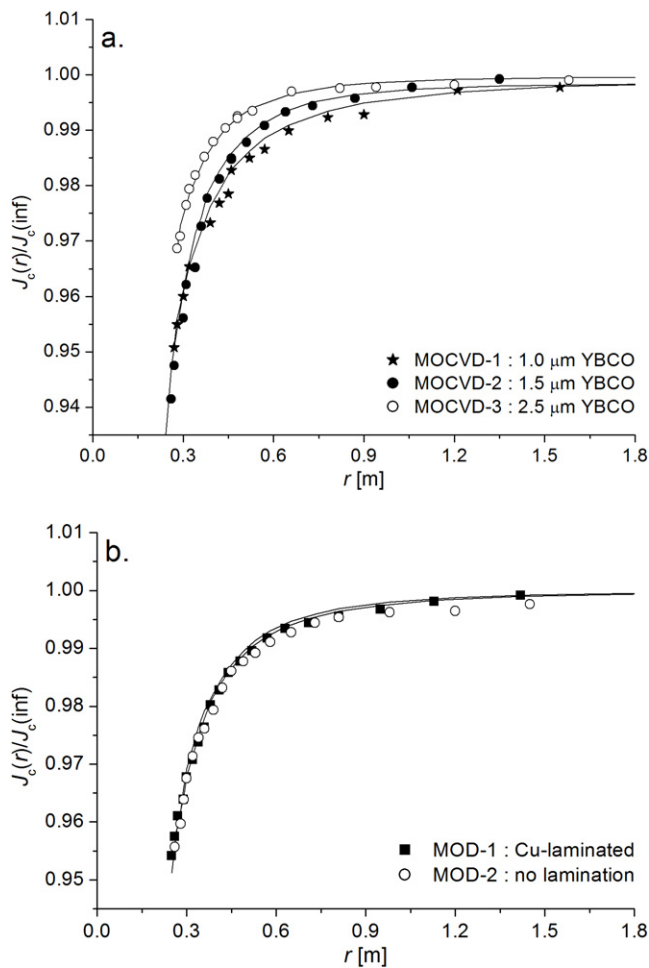


**Figure 6.** Normalized critical current density as a function of in-plane bending radius of (a) MOCVD-IBAD coated conductors with layer thicknesses of 1.0  $\mu\text{m}$  (MOCVD-1), 1.5  $\mu\text{m}$  (MOCVD-2) and 2.5  $\mu\text{m}$  (MOCVD-3) and (b) of MOD-RABiTS coated conductors with (MOD-1) and without (MOD-2) copper laminates. The solid lines are a fit to the data of equation (2).

according to equation (2). The model describes the data very well for all types of samples. The values of the fitting parameters used in the model are also listed in table 2.

The differences between the three samples of figure 6(a) can be explained by the way they were mounted on the bending beam and by the width of their current paths. The neutral axis of the bending beam would be located in the center of the sample when the sample is mounted exactly at the beam center. In that case, parameters  $c$  and  $d$  in expression (1) are equal to half the sample width (2 mm in this case). The values for parameter  $c$ , equal to 1.4 mm, and  $d$ , equal to 2.4 mm, for sample MOCVD-3 suggest that it was mounted off-center. In this situation, the gray area in figure 4 would move slightly towards positive strain and  $J_c$  would be slightly less sensitive to in-plane bending. This is exactly what is observed in figure 6(a) with sample MOCVD-3.

Most samples have an effective width for current flow that is slightly smaller than the physical width of the samples (4 mm). This is caused mostly by the damage done by slitting when the samples were slit to their final width. The width of the current path also has a large impact on the

sensitivity of  $J_c$  to in-plane bending. A narrower sample is less sensitive to in-plane bending than a wider sample, as shown in figure 6(a), when samples MOCVD-2 and MOCVD-3 are compared. Both samples were apparently mounted slightly off-center. Sample MOCVD-2 has an effective width greater than sample MOCVD-3, and thus is more sensitive to in-plane bending.

## 5. Conclusions

A model that predicts the dependence of the critical current density of YBCO coated conductors on in-plane bending has been introduced. The model gives a good description of data obtained on coated conductors, where the critical current density as a function of in-plane bending radius was measured by a new technique. The dependence of the critical current on strain and on in-plane bending does not depend on the thickness of the YBCO layer, which is a promising result for high-current coated conductors with a YBCO layer thickness up to 2.5  $\mu\text{m}$ . The sensitivity of the critical current density of YBCO coated conductors on in-plane bending depends on the dependence of the critical current on axial strain and on the width of the sample. The model also provides for an estimate of the width of the current path. A reversible reduction in critical current density of 4–5% at a critical in-plane bending radius of 0.25–0.28 m has been measured on samples with a width of 4 mm. This presents the critical minimum bending radius, since at smaller bending radii the critical current degradation becomes irreversible. The critical current degrades irreversibly at an in-plane bending radius at which the sample edge under tension exceeds the irreversible strain limit.

Based on the results that are presented in this paper, it is concluded that the dependence of the critical current density on in-plane bending can be estimated in a straightforward manner from the dependence of  $J_c$  on axial strain. A similar calculation can be performed to obtain  $J_c$  for YBCO coated conductors under torsion, or even when a combination of axial strain, torsion, or in-plane bending is applied. The critical current density then simply follows from the spatial integration of  $J_c$ , while taking the distribution in strain over the width of the sample into account. This model greatly simplifies the design of applications, as only the strain distribution and the dependence of  $J_c$  on pure axial strain need to be obtained.

## Acknowledgments

The authors thank SuperPower Inc. and American Superconductor Corporation for providing samples. This work was supported in part by the US Department of Energy, Office of Electricity Delivery and Energy Reliability.

## References

- [1] Selvamanickam V *et al* 2006 *Physica C* **463** 482–7
- [2] van der Laan D C and Ekin J W 2007 *Appl. Phys. Lett.* **90** 052506
- [3] Shin H-S, Choi S-Y, Ko D-K, Ha H-S, Ha D-W and Oh S-S 2003 *IEEE Trans. Appl. Supercond.* **13** 3526–9

- 
- [4] Ekin J W 1980 *Filamentary Al<sub>5</sub> Superconductors* ed M Suenaga and A F Clark (New York: Plenum) pp 187–203
- [5] Selvamanickam V 2001 *IEEE Trans. Appl. Supercond.* **11** 3379–82
- [6] Selvamanickam V, Xie Y, Reeves J and Chen Y 2004 *MRS Bull.* **29** 579–82
- [7] Rupich M W, Verebelyi D T, Zhang W, Kodenkandath T and Li X P 2004 *MRS Bull.* **29** 572–7
- [8] Malozemoff A P *et al* 2008 *Supercond. Sci. Technol.* **21** 034005
- [9] Feldmann D M *et al* 2007 *J. Appl. Phys.* **102** 083912
- [10] Goyal A *et al* 1996 *Appl. Phys. Lett.* **69** 1795–7
- [11] Norton D P *et al* 1996 *Science* **274** 755–7